Available online at www.sciencedirect.com
SCIENCE DIRECT®
Journal of Solid State Chemistry 177 (2004) 1542–1548
JOURNAL OF SOLID STATE CHEMISTRY
http://elsevier.com/locate/jssc

Synthesis of nanocrystalline ytterbium modified $PbTiO_3$

F.C.D. Lemos,[a,*] E. Longo,[a] E.R. Leite,[a] D.M.A. Melo,[b] and A.O. Silva[b]

[a] *Centro Multidisciplinar para o Desenvolvimento de Materiais Cerâmicos (CMDMC), Departamento de Química, Universidade Federal de S. Carlos, SP 13565-905, Brazil*

[b] *Departamento de Química, UFRN, P. O . Box 1662, Natal, RN 59078-970, Brazil*

Received 22 August 2003; received in revised form 1 December 2003; accepted 9 December 2003

Abstract

Ytterbium (Yb) modified lead titanate ceramics ($Pb_{1-x}Yb_x\ TiO_3$, with $x = 0.05$) (PYbT) were prepared by the Pechini method. The materials were calcinated under flowing oxygen at different temperatures from 300°C to 700°C. Nanostructured PYbT was obtained by high-energy milling and investigated using X-ray diffraction (XRD), thermogravimetric analysis (TGA), differential thermal analysis (DTA), transmission electron microscopy (TEM), scanning electron microscopy (SEM) and surface area analysis (BET). The results revealed that the obtained materials are formed by nanometric particles.

Keywords: $PbTiO_3$; Rare earth; Perovskite; Pechini method

1. Introduction

$PbTiO_3$ (PT) with tetragonal perovskite structure at room temperature, is a ferroelectric compound with Curie temperature of 490°C, high pyroelectric coefficient, high spontaneous polarization and low dielectric constant [1]. Some authors have investigated PT materials modified by various additives [2–5]. Lead titanate (PT) ceramics modified by rare earth elements and alkaline earth elements are extremely good for high frequency applications [6]. The properties of these ceramics are strongly related to stoichiometry. The presence of intermediate phases can significantly damage the electrical properties [7]. The formation of lead deficient phases delay and even hinder the formation of perovskite [8]. Sirera and Calzada [9], upon obtaining pure and doped PT powders, observed the emergence of a pyrochlore phase which disappeared with the increase of the treatment temperature.

Nanostructured PT can be obtained by different methods [10]. High-energy milling is an alternative method of processing amorphous or nanostructured PT [11,12]. This process is widely used in the preparation of nanostructured metals and alloys [13] and has been applied to the production of nanostructured ceramic materials [14,15]. In this paper we report XRD, thermal analysis (TG and DTA), TEM, SEM and BET [16] data for nanostructured ytterbium-modified lead titanate ceramics obtained by high-energy milling.

2. Experimental procedure

2.1. Synthesis

Initially modified PT ceramics were prepared from highly pure starting materials, using the so-called polymeric precursor method proposed by Pechini [17]. Lead (II) acetate trihydrate $[Pb(CH_3COO)_2 \cdot 3H_2O]$, Ytterbium oxide ($Yb_2O_3$) and titanium (IV) isopropoxide $Ti[OCH(CH_3)_2]_4$ were used as starting materials. Ethylene glycol and citric acid were used as polymerization/complexation agents for the process. Ammonium hydroxide was used to adjust the pH and so preventing lead citrate precipitation.

Titanium citrates were formed by the dissolution of titanium IV isopropoxide in an aqueous solution of citric acid (60–70°C). After the homogenization of the Ti-citrate solution ($0.015\,mol\,L^{-1}$), a stoichiometric amount of $[Pb(CH_3COO)_2 \cdot 3H_2O]$ was dissolved in

*Corresponding author. Fax: +84-211-9224.
E-mail address: p-fcdl@iris.ufscar.br, lemos@materiais.ufrn.br (F.C.D. Lemos).

0022-4596/$ - see front matter © 2003 Elsevier Inc. All rights reserved.
doi:10.1016/j.jssc.2003.12.005

water and soon thereafter added to the Ti-citrate solution, which was kept under slow agitation until a clear solution was obtained. In the preparation of the ytterbium solution, Yb_2O_3 was first by dissolved in nitric acid and gradually added to the Pb–Ti-citrate solution. To achieve total dissolution of the cations, ammonium hydroxide was dropwisely added until the pH reached 6–7. The complete dissolution of the salts resulted in a clear solution.

After homogenization of the solution containing the Pb and Yb cations, ethylene glycol was added to promote mixed citrate polymerization by the polyesterification reaction. Upon continued heating at 80–90°C, the solution became more viscous, without any visible phase separation. The molar ratio among lead–ytterbium and titanium cations was 1:1, the citric acid/metal molar ratio was fixed at 1.00, and the citric acid/ethylene glycol mass ratio was fixed at 60/40.

The heat-treatment temperature of the polyester resin thus obtained must be sufficient to promote the polymer pyrolysis, without crystallization. The resulting porous material was easily de-agglomerated in a mortar and next it was heat-treated at different temperatures in an oxygen atmosphere for 2 h. The heat-treatment process was accompanied by XRD, SEM, thermal analysis (TGA and DTA), BET and TEM analysis.

Ultrafine PYbT obtained at 700°C, presenting only one phase, was mechanically milled in a high-energy attrition mill for 1 h and analyzed by SEM, BET and TEM.

2.2. Characterization

2.2.1. X-ray diffraction

The calcined material was evaluated by X-ray diffraction (XRD) using Cu$K\alpha$ radiation in a Siemens D5000 apparatus. The diffraction angle (2θ) ranged between 5° and 75°.

2.2.2. Transmission electron microscopy (TEM)

PYbT powder was de-agglomerated in an aqueous solution using an ultrasound probe. A drop of this solution was dripped over a carbon-covered copper net before being introduced in the sample holder for TEM imaging (Phillips CM 200).

2.2.3. Scanning electron microscopy (SEM)

SEM micrographs were recorded with the help of a Zeiss DSM940A microscope.

2.2.4. Nitrogen adsorption/desorption (BET)

The surface area was determined by means of the BET multi-point method and an ASAP 2000 equipment was used for the adsorption/desorption analysis.

2.2.5. Thermal analyze

The TGA analyses were carried out in a TGA-50 Schimadzu balance using a 7 mg sample mass in a platinum sample holder, heating rate of $10°C\,min^{-1}$ under dynamic air atmosphere ($50\,mL\,min^{-1}$) in the temperature range of 30–800°C. DTA analyses were obtained under the same conditions in a DTA 1700 Perkin-Elmer apparatus.

3. Results and discussion

3.1. X-ray diffraction

To study the phase development with increasing calcination temperature, the materials were calcinated for 2 h under flowing oxygen at various temperatures, up to 700°C, followed by phase analysis using XRD. Figs. 1 and 2 show the XRD patterns of powders at various calcination temperatures for the pure PT and PYbT, respectively. At 300°C it was observed that both pure PT and PYbT are amorphous and above this temperature the tetragonal phase is obtained for the pure PT while a mixture of phases for the PYbT is observed. For the PYbT sample, one can notice two peaks around $2\theta = 30.4°$, 60.4° and one peak around $2\theta = 35.3°$, which are believed to be due to the PbO and pyrochlore or flurite phase respectively, when it was calcinated at 400°C, 500°C and 600°C. Intermediate phases, related to PbO or to the pyrochlore phases, were converted to tetragonal phase, with increasing temperature [18]. Increasing the calcination temperature up to 700°C

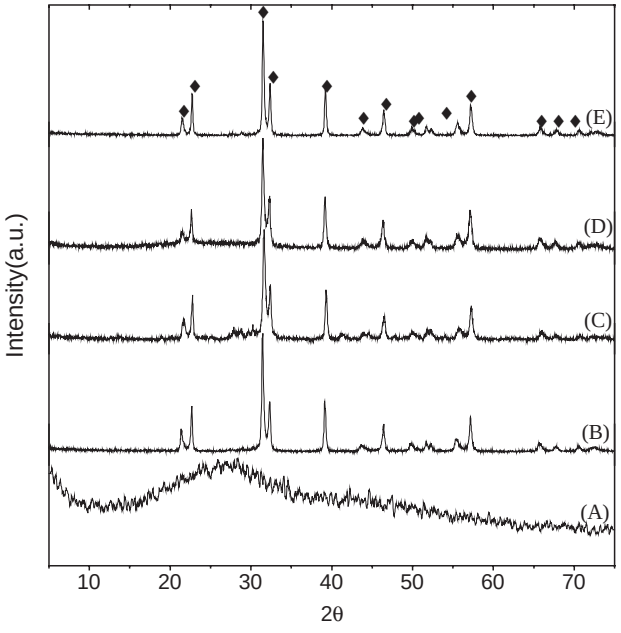

Fig. 1. XRD analysis of the pure PT powders, calcined for 2 h under flowing oxygen at various temperatures. A–E at 300°C, 400°C, 500°C, 600°C and 700°C, respectively (◆, tetragonal phase).

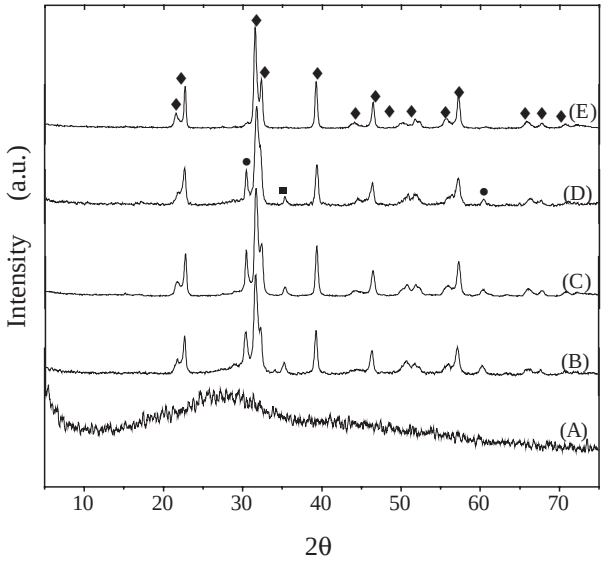

Fig. 2. XRD analysis of the PYbT powders, calcined for 2 h under flowing oxygen at various temperatures. A–E at 300°C, 400°C, 500°C, 600°C and 700°C, respectively (◆, tetragonal phase; ●, PbO; ■, fluorite phase).

resulted in a further development of the tetragonal phase and most of the intermediate phases were eliminated.

3.2. Thermal analysis

Figs. 3a, b and 4a, b present the TGA curves and DTA curves of the PT and PYbT precursors, respectively. The TGA curves of the PT (Fig. 3a) and PYbT (Fig. 3b) are similar showing three-stage weight loss, a steady weight loss from room temperature up to 200°C, a slow weight loss over the temperature range from 250°C to 460°C and a sharp fall in the specimen weight over the temperature range from 460°C to 530°C for both materials. Little weight loss is observed at temperatures above 530°C, indicating the completion of all the reactions involving weight loss. The weight loss below 200°C is probably due to the elimination of residual water and the dehydration in the precursors which can be associated with an endothermic peak in the temperature range 70–180°C, as well as the volatilization of excess ethylene glycol for both precursors. The slow weight loss and the fall in the specimen weight over the temperature range from 250°C to 530°C is related to the oxidative decomposition of the organic material (Fig. 4) along the broad exothermic peak from 260°C to 380°C for the PT precursor (Fig. 4a) and from 260°C to 362°C for the PYbT precursor (Fig. 4b). The peaks located at 390°C and 378°C for the PT and PYbT precursors, respectively are due to the crystallization of the remaining PbO and the subsequent conversion to the perovskite phase, according to XRD results (Figs. 1 and 2). There is a peak in the plots of Fig. 4 around

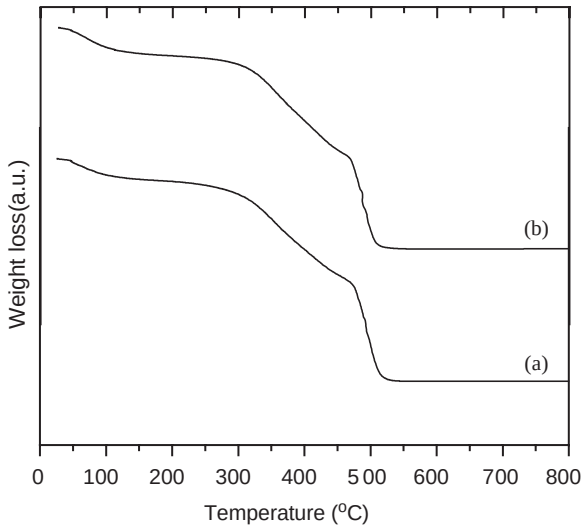

Fig. 3. TGA of PT (a) and PYbT (b) citrate polymeric precursors.

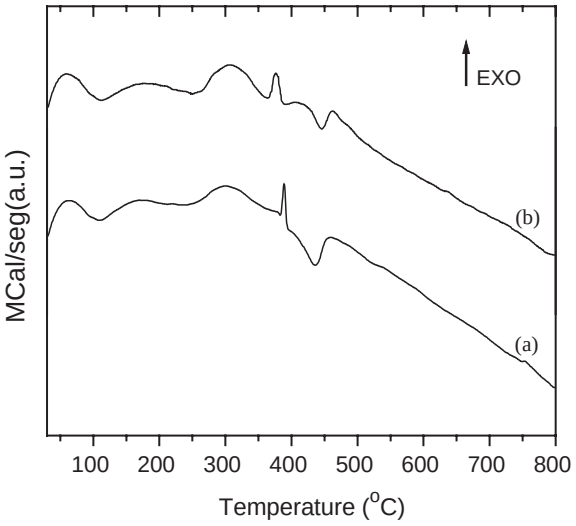

Fig. 4. DTA of PT (a) and PYbT (b) citrate polymeric precursors.

461°C for both materials, which is suggestive of the transformation of the cubic phase to the tetragonal phase.

3.3. Morphology of powders

The PYbT powders obtained present more than one phase, in agreement with what has been revealed by XRD. Fig. 5 shows three SEM micrographs revealing the microstructure of powders calcinated under flowing oxygen at 600°C and 700°C for two hours without mechanical treatment and at 700°C after mechanical treatment. In Fig. 5A a porous aspect it is observed in some areas of the sample, as well the presence of crystallites. At 700°C (Fig. 5B) the presence of small crystallites and agglomerates of particles is observed,

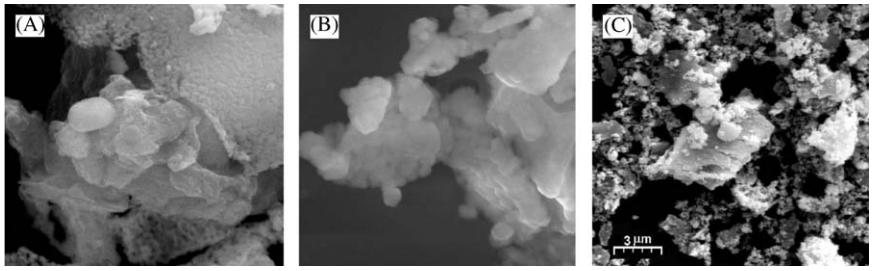

Fig. 5. SEM micrographs of PYbT powders, (A) before mechanical treatment and calcined at 600°C. (B) Same calcined at 700°C. (C) after mechanical treatment, calcined at 700°C.

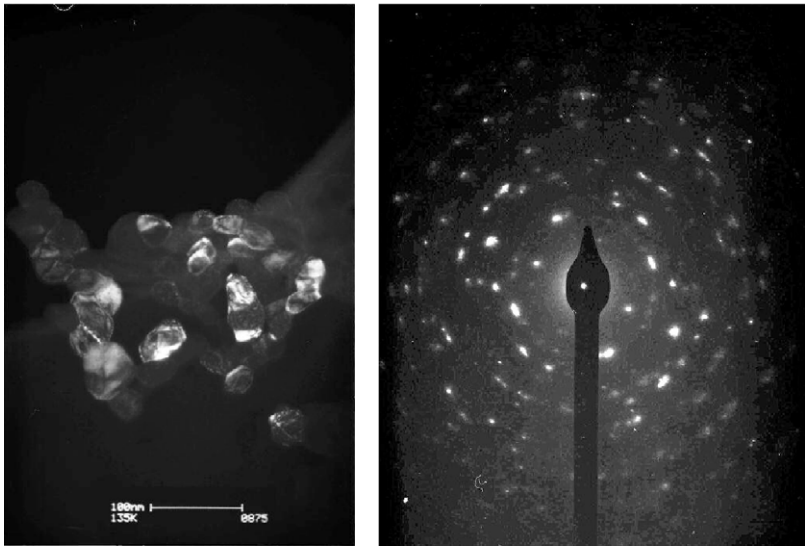

Fig. 6. TEM micrograph of PYbT powders before mechanical treatment.

what suggests the existence of a mixture of phases. The PYbT obtained at 700°C, which presented one phase, was mechanically treated in a high-energy attrition mill for 1 h. The ultrafine PYbT powder, mechanically milled, presents the same morphology of the material without the mechanical treatment, according to the SEM micrographs, however, there is a dramatic fall in the crystallite size (Fig. 5C).

Figs. 6 and 7 show the TEM micrograph together with the selected area diffraction patterns for the powders before and after mechanical treatment, respectively. In the TEM micrographs of the material without mechanical treatment (Fig. 6), it is observed that the particle morphology is similar and the size of the crystallites is around 50 nm. The established multi-spot rings of selected area diffraction patterns clearly indicate the polycrystalline nature of the powder. Conversely, the micrographs of the mechanically treated powders (Figs. 7A and B) indicate that these powders are agglomerates of nanocrystalline and amorphous phases, although visible agglomerates of particles in the micrometric scale are observed (Fig. 8). This suggests that a certain degree of amorphization occurred, as the powder was mechanically treated. The ultrafine PYbT powders obtained through the use of the mill presents crystallite sizes smaller than those obtained for the material without mechanical treatment (Figs. 7A and B).

The phase formed before perovskite has been frequently described as the fluorite phase, but they will be formed simultaneously [19]. Charles et al. [20] obtained parameters in their work during the development of the titanate synthesis, that evidenced the presence of the fluorite phase and they did not observe the presence of the pyrochlore phase. In the present study, the r values (Table 1), calculated from the selected area electron diffraction (SAED) TEM, supplied values of the lattice space for an intermediate phase. Since in our diffraction data there is no presence of the cell-doubling reflections (d_{111} and d_{311}) from the face-centered pyrochlore [21,20], we suggest that the intermediate phase present the fluorite-type structure.

The control of particle morphology is one of the main objectives for the non-conventional synthesis method of ceramic powders. The characterization of particle

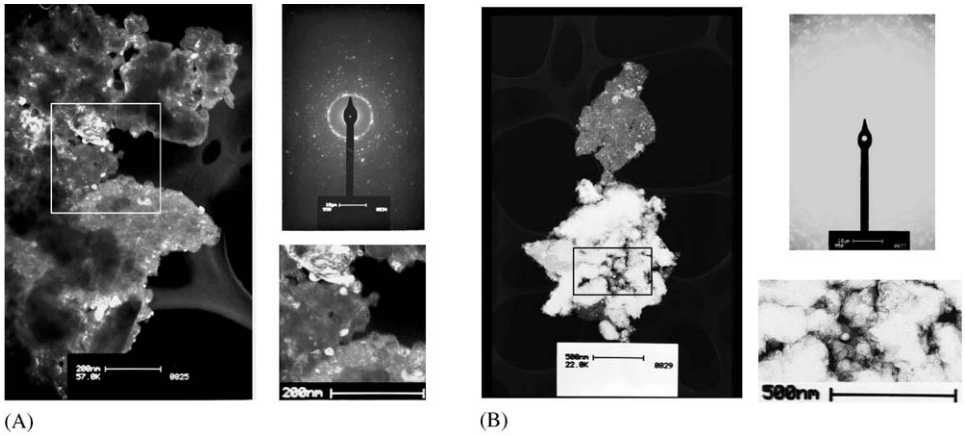

Fig. 7. TEM micrographs of PYbT powders after mechanical treatment. (A) Micrographs and diffraction pattern for the area of nanometric particles and (B) for the area of larger particles.

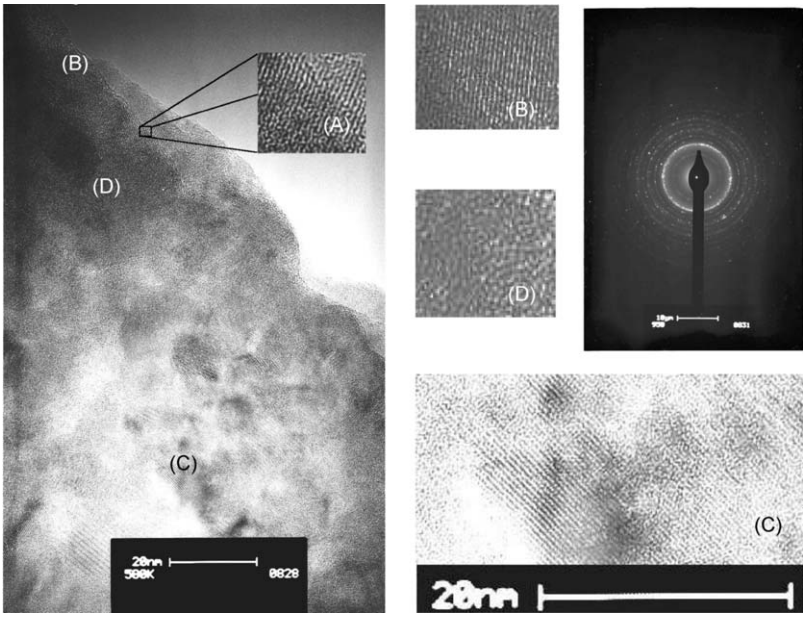

Fig. 8. High resolution transmission electron photomicrographs of mechanically treated PYbT powders, with indication for crystalline (A), (B), (C) and amorphous (D) areas.

morphology normally involves the measurement of specific surface area, and pore and particle size distribution by using the technique of isothermal gas adsorption and desorption. The use of this technique provides the analysis of pore morphology, from sub-nanometric dimensions (<0.5 nm) until approximately 180 nm, being especially indicated for the study of catalysts and ceramic materials prepared from ultrafine powders [22,23]. Several theoretical treatments exist for the calculation of the superficial area through gaseous adsorption. In this present work we used the BET treatment. The ultrafine PYbT powders, before and after mechanical treatment submitted to the BET analysis are shown in Fig. 9. The analysis of the plots in Fig. 9 shows a type II isotherm [23,24] indicating the presence of mesopores (pores with a diameter of 2–100 nm) and a H−1 hysteresis [23,25]. The H−1 hysteresis suggests the presence of agglomerates with cylindrical pores for both powders. Table 2 shows results of surface areas (S_{BET}) and mean crystallite sizes by BET. This table shows that the mean particle size of the milled powders is smaller than those obtained without the mechanical treatment.

4. Conclusions

Polycrystalline ytterbium-modified lead titanate powders obtained by the polymeric precursor method were successfully prepared. The perovskite single phase

Table 1
Comparison of lattice parameters calculated from SAED patterns based on macedonite, fluorite and cubic pyrochore structure

Macedonite[a] (*hkl*) and *d* (nm)	Fluorite[a] (*hkl*) and *d* (nm)	Pyrochlore[a] (*hkl*) and *d* (nm)	Present work (*hkl*) and *d* (nm)
PYbT before milled			
(100) 3.90			(100) 3.90
(110) 2.76	(200) 2.73		(110) 2.77
(111) 2.29			(111) 2.26
(200) 1.95	(220) 1.93		(200) 1.91
(211) 1.60			(211) 1.59
(003) 1.38	(400) 1.36		(003) 1.38
PYbT after milled			
(001) 4.15			(001) 4.02
(101) 2.84			(101) 2.86
(111) 2.29			(111) 2.26
(200) 1.95	(220) 1.93	(511) (333) 1.95	(200) 1.94
(201) 1.76			(201) 1.76
(211) 1.60	(222) 1.57		(211) 1.59

[a] Crystallographics informations obtained from ICSD (Inorganic Crystal Structure Database).

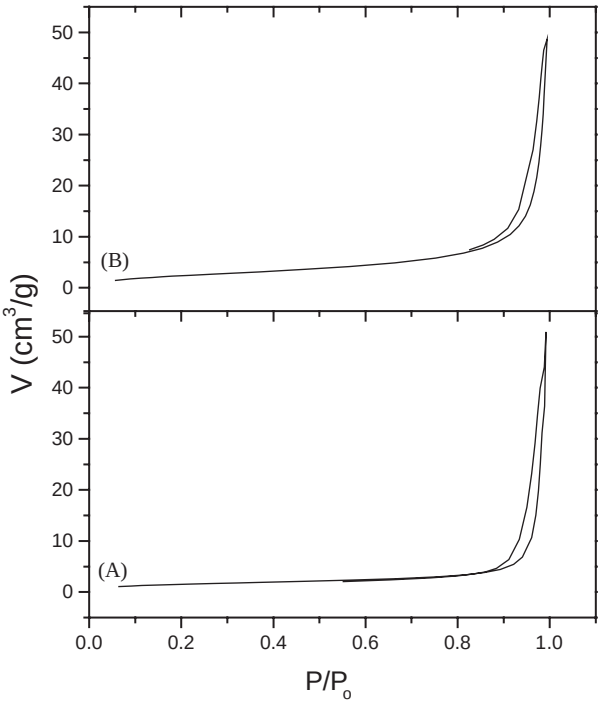

Fig. 9. Nitrogen adsorption/desorption isotherms for pure PT (A) and PYbT powders (B).

formation, as was observed at a temperature above 300°C for the pure PT and above 600°C for the PYbT, respectively determined by DRX. These results suggest that the modifier cation incorporated into the system has notable influence in the microstructure and cystallinity of lead titanate powders and also favors the occurrence of a second phase, identified as fluorite according with the obtained TEM results.

Table 2
Morphologic characteristcs of the PYbT particles, before and after the mechanical treatment

Sample	S_{BET} (m^2/g)	D_{BET} (nm)
PYbT before mechanical treatment	5.5891	134
PYbT after mechanical treatment	9.4479	79

The analyses of TEM showed that the crystallite sizes is around 50 nm without the use of the mechanical treatment. For the mechanically treated material there is a notable decrease in the crystallite sizes, what was qualitatively confirmed by the nitrogen adsorption/desorption curves. These results demonstrate the feasibility of the milling process of obtaining adequate nanometric particles.

Acknowledgments

The authors gratefully acknowledge the financial support of the Brazilian research funding agencies FAPESP, CNPq, PRONEX and CAPES.

References

[1] T. Fukuit, J. Sol–Gel Sci. Tech. 11 (1998) 31.
[2] R. Sirera, M.L. Calzada, Mater. Res. Bull. 30 (1) (1995) 11.
[3] J. Ricotea, E. Snoeck, R. Coratger, L. Prado, J. Phys. Chem. Solids 59 (2) (1998) 151.
[4] F.M. Pontes, J.H.G. Rangel, E.R. Leite, E. Longo, J.A. Varela, E.B. Araújo, J.A. Eiras, J. Mater. Sci. 36 (2001) 3565.
[5] D.S.L. Pontes, E.R. Leite, F.M. Fontes, E. Longo, J. Mater. Sci. 36 (2001) 3461.
[6] R. Tickoo, R.P.Tandon, N.C. Mehra, P.N. Kotru, Mater. Sci. Eng. B 94 (2002) 1.
[7] J. Tartaj, C. Moure, P. Durán, Ceram. Int. 27 (2001) 741.
[8] J. Tartaj, J.F. Fernández, M.E. Villafuerte-Castrejón, Mater. Res. Bull. 36 (2001) 479.
[9] R. Sirera, M.L. Calzada, Mater. Res. Bull. 30 (1995) 11.
[10] P.S. Pizani, E.R. Leite, F.M. Pontes, E.C. Paris, J.H. Rangel, E. Lee, E. Longo, P. Delega, J.A. Varela, Appl. Phys. Lett. 77 (6) (2000) 824.
[11] E.C. Paris, E.R. Leite, E. Longo, J.A. Varela, Mater. Lett. 37 (1998) 1.
[12] E.R. Leite, L.P.S. Santos, N.L.V. Carreño, E. Longo, C.A. Paskocimas, J.A. Varela, F. Lanciotti Jr., C.E.M. Campos, P.S. Pizani, Appl. Phys. Lett. 78 (15) (2001) 2148.
[13] H. Bakker, G.F. Zhou, H. Yang, Prog. Mater. Sci. 39 (1995) 159.
[14] J. Wang, D.M. Wan, J.M. Xue, E.B. Ng, Adv. Mater. 11 (3) (1999) 210.
[15] J. Subrt, L.A. Perez-Maqueda, J.M. Criado, C. Real, J. Bohacek, E. Vecernikova, J. Am. Ceram. Soc. 83 (2000) 294.
[16] S. Brunauer, P.H. Emmett, E. Teller, J. Am. Chem. Soc. 60 (1938) 309.
[17] M. Pechini, US Patent No. 3.330.697, 1967.
[18] J. Fang, J. Wang, Leong-Ming Gan, Ser-Choon Ng, Mater. Lett. 52 (2002) 304.

[19] A.H. Carim, B.A. Tutlle, D.H. Doughty, S.L. Martinez, J. Am. Ceram. Soc. 74 (6) (1991) 1455.
[20] C.D.E. Lakeman, Zhengkui Xu, D.A.Payne, J. Mater. Res. 10(8) (1995) 2042.
[21] J. Ricotea, E. Snoeck, R. Coratger, L. Pardo, J. Phys. Solids 59 (2) (1998) 151.
[22] E.R. Leite, J.A. Varela, E. Longo, C.A. Paskocimas, Ceram. Int. 21 (1995) 153.
[23] C.V. Santilli, S.H. Pulcinelli, Cerâmica 39 (1993) 259.
[24] S. Brunauer, L.S. Dening, W.S. Dening, E. Teller, J. Am. Chem. Soc. 62 (1940) 1723.
[25] K.S.W. Sing, Pure Appl. Chem. 54 (11) (1982) 2201.